BioNanoScience (2022) 12:1086–1096
https://doi.org/10.1007/s12668-022-01035-4

Antimicrobial and Detoxification Study of Novel Luminescent CuO Nanoparticles Synthesized by White Garland Lily Leaves Extract

P. B. Nagore[1] · A. J. Ghoti[1] · A. P. Salve[1] · K. G. Mane[1]

Accepted: 10 September 2022 / Published online: 26 September 2022

Abstract

The novel luminescent copper oxide nanoparticles (CuONPs) were furnished by using white garland lily leaves extract. The method for this synthesis was economical, simple, environment friendly, and importantly followed green chemistry principles for the development of a proficient approach in the arena of biological applications and detoxification of industrial-grade toxic dye. The characterization study of CuONPs was done by UV–Visible, FT-IR, XRD, HRTEM, FESEM-EDAX, and PL spectra. The particle size (average) revealed by XRD, HRTEM, and FESEM analysis was 40 ± 0.5 nm. The O.D. around 300 nm in UV–Vis spectra established the effective synthesis of CuONPs while the peaks around 295 and 590 nm in PL spectra revealed its luminescence property. The novel CuONPs were verified against the selected bacterial and fungal strains. The CuONPs exhibited outstanding antibacterial activities versus *E. coli* and *S. Pyogenus* while having considerable antifungal activities against selected fungal strains. Moreover, the CuONPs were tested for photocatalytic degradation proficiency against methylene blue (MB) and found effective even after three cycles (100% removal in 70 min). The photocatalytic efficacy and its high reusability in consort with great adaptability of economic green synthesis favor the practice of novel CuONPs as a hopeful choice for the detoxification of natural resources poisoned with industrial dye.

Keywords Green method · Nanotechnology · White garland lily, Plant leaves

1 Introduction

The present epidemic has asked for an urgent alternative to search for human antimicrobial resistance (AMR) and the cleaning of natural resources. Unfortunately, the AMR has emerged as a severe threat as the microbes show mutations, leading to the failure of existing antimicrobial agents, causing huge loss of human lives with economy [1, 2].

Nowadays, nanotechnology and nanoscience have arisen as the future technology for life. Researchers worldwide are working on the enrichment of the nanoworld. In that context, people are working on newer nanoparticle synthesis methods apart from existing methods. Biological methods, especially using plants and secondary metabolites for nanoparticle synthesis, have been the budding area for researchers worldwide owing to many benefits over existing methods [3–7].

Copper, a metal of the first transition series, is a key element for the kingdom Animalia. There we find ample studies on the phytofabrication of CuONPs [8–15]. White garland lily, also called ginger lily (Fig. 1), is a plant from the family Zingiberaceae and is a perennial ornamental species known for its beautiful white flowers used as garland flowers in Maharashtra. *Hedychium coronarium* Koenig is the botanical name of this species. It has some significant medicinal properties like antimicrobial, antioxidant, anti-hypertensive, and antimalarial potentials [16, 17].

This article presents an eco-benevolent, simple phytofabrication of CuONPs, employing white garland lily leaves extract (WGLLE), its antibacterial and antifungal activities along with its photocatalytic efficacy. To date, this plant is being utilized only for AgNP synthesis, using rhizome extract [18]. So, this article devotes the phytosynthesis of CuONPs with WGLLE, for the first time.

✉ K. G. Mane
kanchanmane13@gmail.com

[1] M.T.E.S's, Doshi Vakil Arts College and G.C.U.B. Science & Commerce College, Goregaon-Raigad, Maharashtra, India

Fig. 1 White garland lily plant

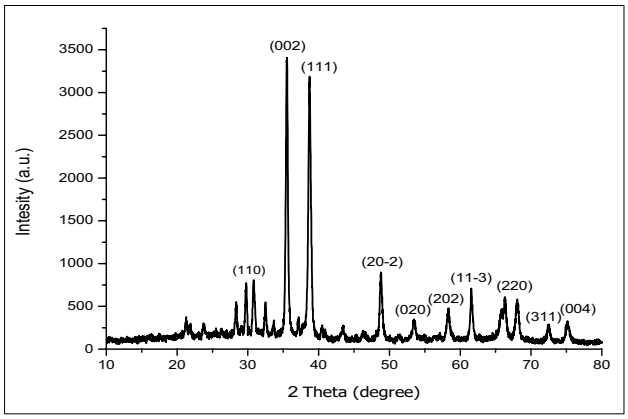

Fig. 3 XRD pattern of WGLLE mediated CuONPs

2 Experimental

2.1 Materials

$CuSO_4.5H_2O$ (AR grade), $NaHCO_3$ (AR grade), and other chemicals were purchased from Molychem, Mumbai, India, and utilized as such.

2.2 Plant Recognition and WGLLE Preparation

The plant recognition was done by Mr. Amol Salve, based on its characteristics explained in Flora of Maharashtra [19]. The specimen was submitted to the Botany department. Freshly collected leaves (20 g) were carried from a household plot belonging to Mr. Satish Doshi, a retired headmaster located at Goregaon. Then, leaves were washed in the laboratory, first by tap water followed by double-distilled water to remove worthless material, and then sliced into very fine bits. These bits were transferred into a 250-mL beaker for boiling, containing 200 mL of double-distilled water for an hour using a hot plate. After an hour mixture

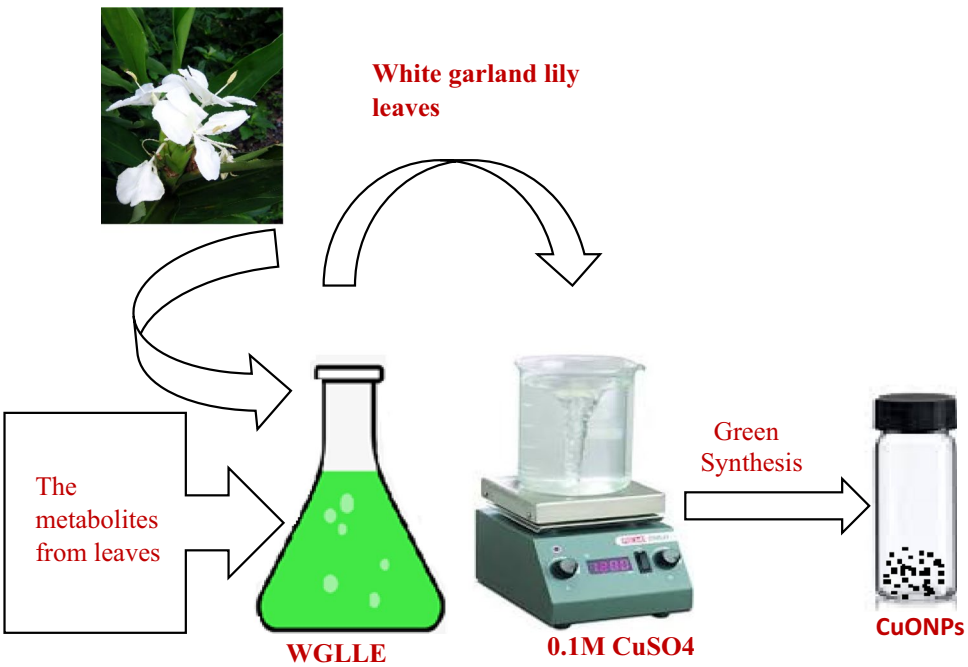

Fig. 2 Diagrammatic representation- Synthesis of CuONPs

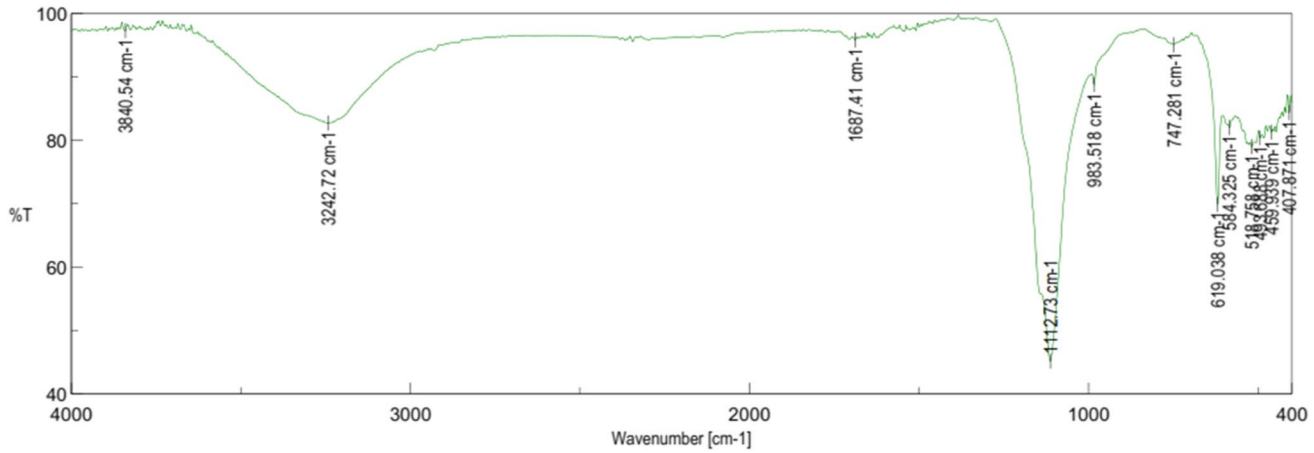

Fig. 4 FT-IR spectra of CuONPs

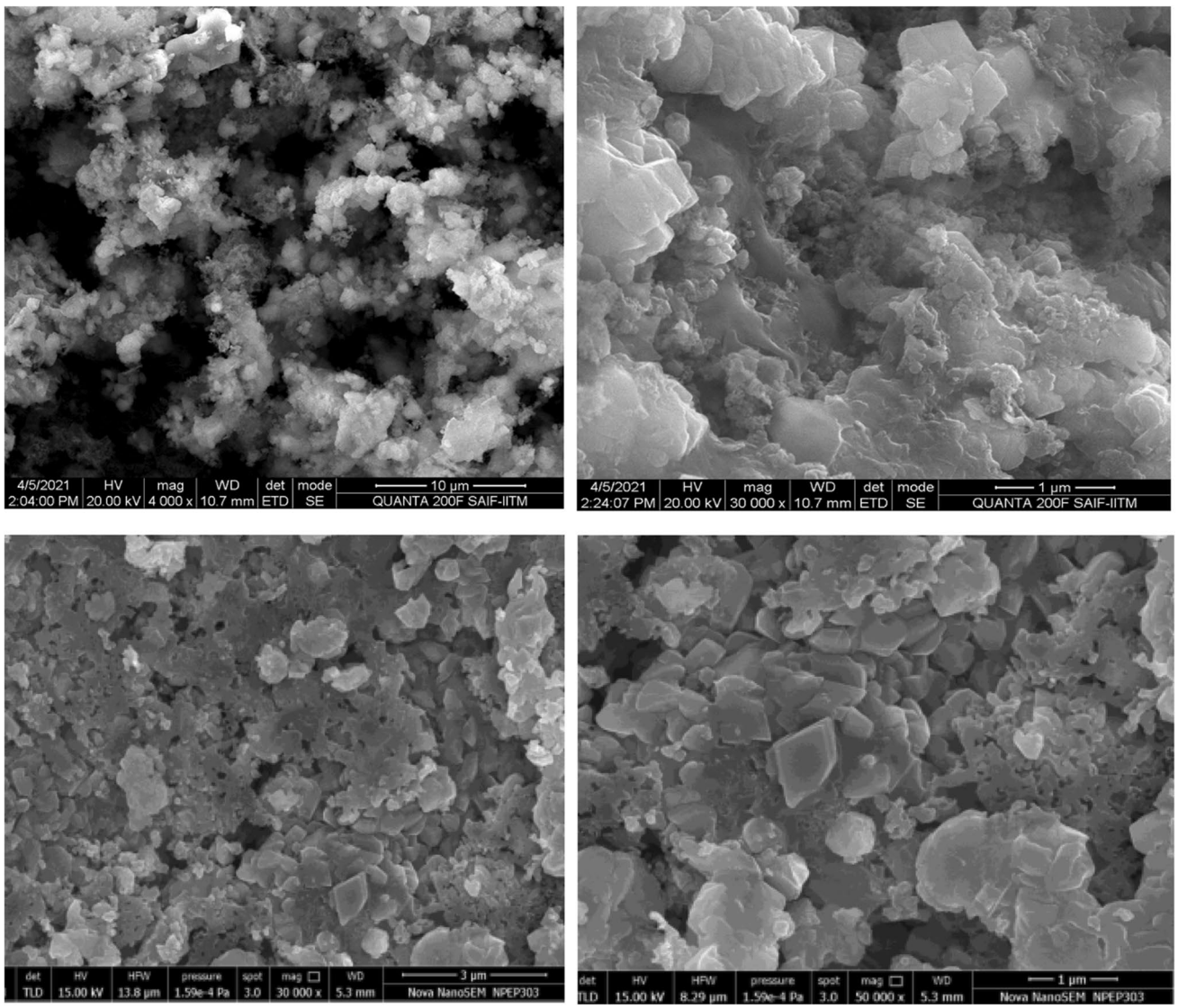

Fig. 5 FESEM images of CuONPs

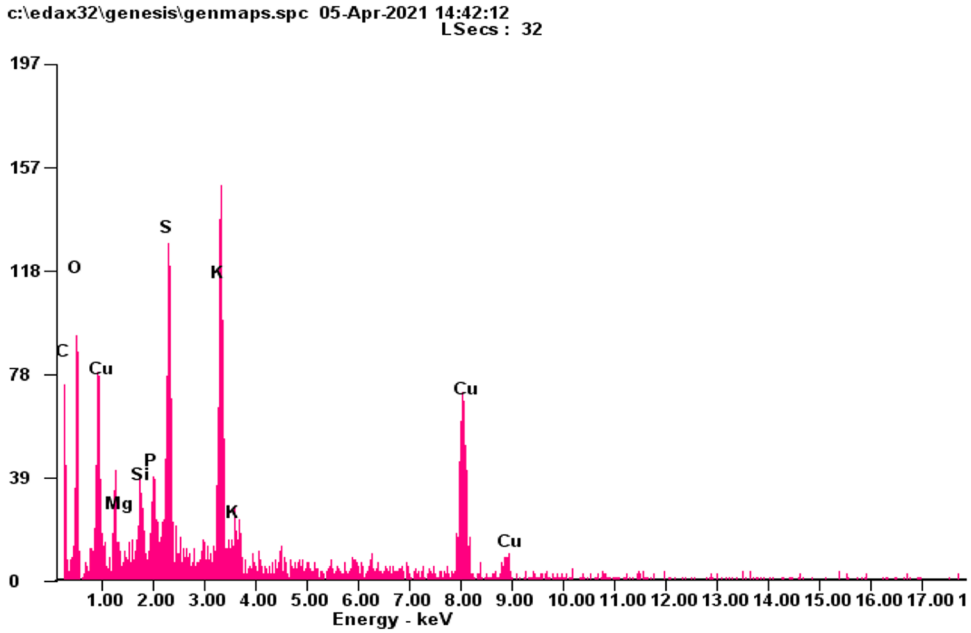

Fig. 6 EDAX spectrum of CuONPs

was double filtered by ordinary and then by Whatman paper no.1 to get white garland lily leaves extract (WGLLE). The WGLLE was stored in a refrigerator until further use.

2.3 Synthesis of CuONPs

The freshly made 0.1 M $CuSO_4{\cdot}5H_2O$ solution with pH 4.6 was mixed to WGLLE in 1:4 ratios, obtained after optimization, which led to an instant alteration in color from green to dark green, which further turned black after stirring on a magnetic stirrer for the 50 min at 500 RPM [8]. The black-colored solid received was then centrifuged at 3500 RPM for around 45 min. After that, it was exposed for combustion in a muffle furnace at around 450 °C. Finally, it was gathered and preserved in a sample tube until further use at the final stage (Fig. 2).

2.4 Characterization Techniques

The UV–Vis spectrum of CuONPs was recorded by Spectrophotometer (Model-JASCO V-770). Functional groups and chemical composition were analyzed by FT-IR (4600 TypeA D044761786) while PL spectra was recorded by spectrofluorometer (Model No. FP-8200, Sr.No.-C026661448). The XRD spectra were recorded by X-ray diffractometer (XRD, Bruker, D8-Advanced Diffractometer) using Cu-Kα radiation ($\lambda = 0.154$ nm) at 40 kV and 40 mA in the range 10–80. High-resolution transmission microscopy analysis was carried out with Model-JEM 200F, accelerating potential: 120 kV and 200 kV. The HRSEM-EDS (FEI Quanta, FEG-200) was used to record the exact size, shape, and elemental composition of CuONPs.

2.5 Phytochemical Screening

The active phytometabolites present in WGLLE were investigated following standard protocols [20].

2.6 Antibacterial Activities

The broth dilution method was used to evaluate the antibacterial efficacy of CuONPs [21, 22] with diluent as DMSO [23–25]. Two $G+$ve and two G –ve bacteria were tested in the experiment. The MIC was taken to the concentration which showed at least 99% inhibition. The results are displayed after triplicate analysis.

2.7 Antifungal Activities

The CuONPs were evaluated versus particular fungal strains using agar dilution protocol following Wiegand et al. [22]. The MIC was considered to be the concentration displaying minimum 99% inhibition with griseofulvin and nystatin as reference drugs. The results were tabulated after triplicate analysis.

2.8 Detoxification Study

This was carried out with MB dye. The 0.25 gm of CuO photocatalyst was dispersed in different concentrations of dye used viz., 1000, 750, 500, 250 ppm and stirred in dark for half an hour to achieve the adsorption–desorption equilibrium mechanism. Then, the solution was exposed to solar radiation and O.D. was recorded after every 10 min.

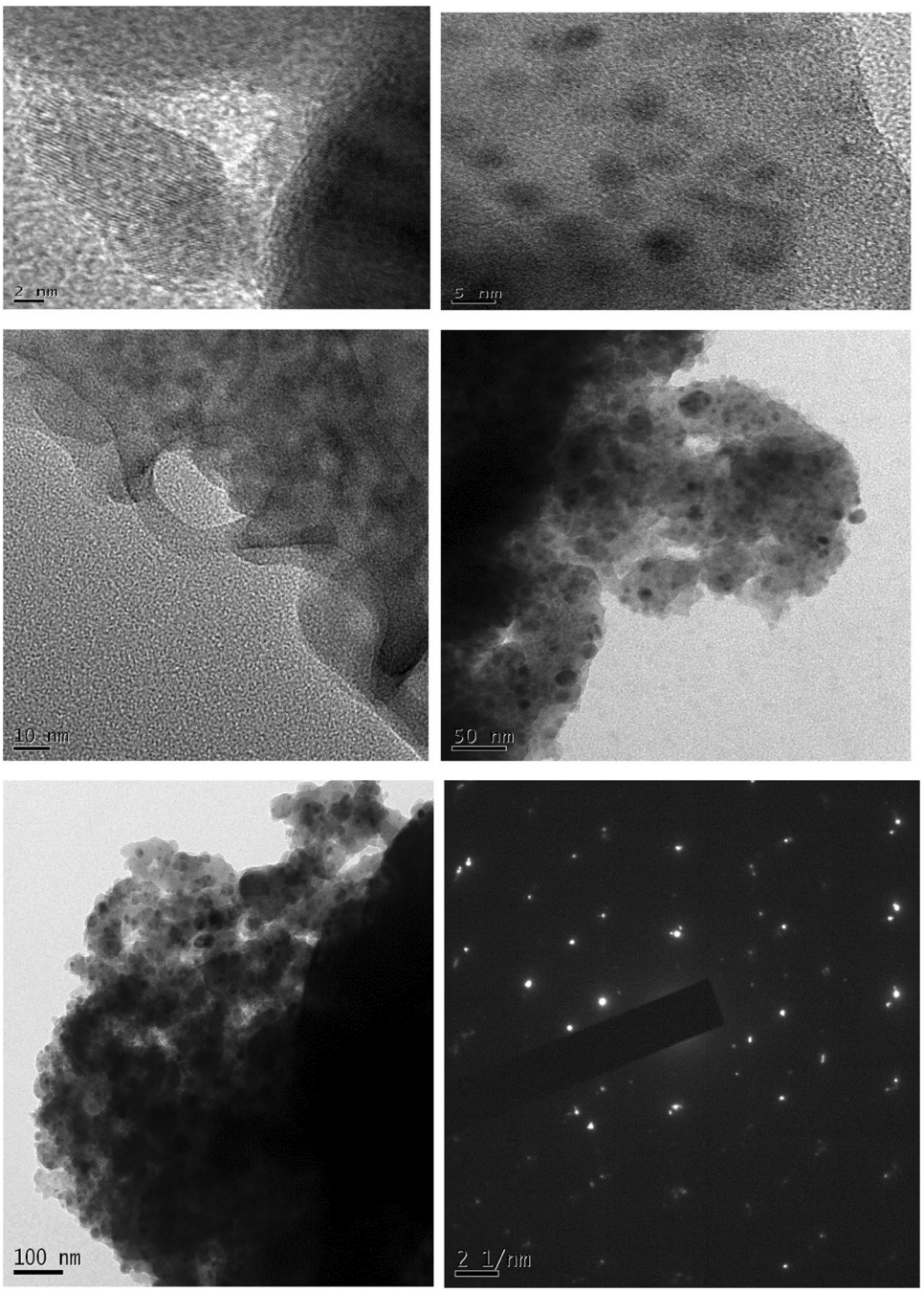

Fig. 7 HRTEM images and SAED pattern of CuONPs

3 Results and Discussion

3.1 The Structural and Crystallographic Analysis

The phytofabricated CuONPs were shiny black in color. The structure and crystallinity of CuONPs fabricated from WGLLE had been examined by XRD patterns as shown in Fig. 3. A powder XRD was carried out using monochromatic CuKα1 28radiation (wavelength 1.5406 Å), in the angular range 2θ of 20°–80° operating at a voltage of 40 kV and a current 40 mA. XRD profile analysis revealed a series of prominent diffraction peaks at 32.48°, 35.54°, 38.72°, 48.8°, 53.48°, 58.32°, 61.58°, 68.6°, 72.38°, and 75.16° which corresponds to (110), (002), (111), (20–2), (020), (202), (11–3), (220), (311), and (004) sets of planes respectively. Also, some unidentifiable peaks can be seen attributed to some organic content or amorphous impurities. The observed sets of planes are indexed based on the monoclinic structure of CuO by comparing the data from JCPDS card No.48–1548. Due to the monoclinic structure of CuO,

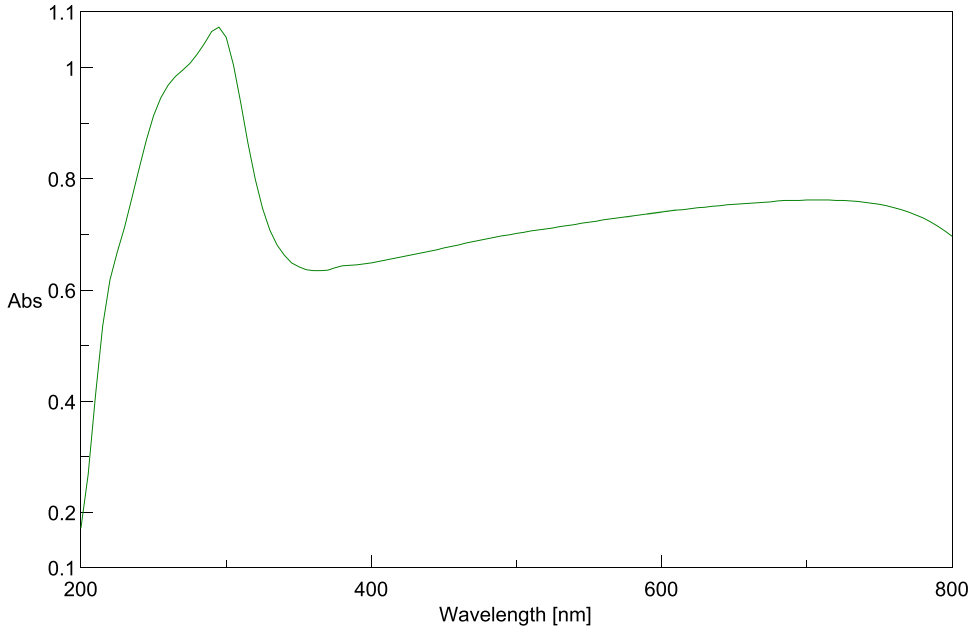

Fig. 8 UV–Visible spectra of CuONPs

the XRD profile analysis thus clearly illustrated that the phytogenically synthesized CuONPs are good crystalline in nature with high purity. The particle size (average) of phytogenically synthesized CuONPs was 40 ± 0.5 nm, calculated using Debye–Scherrer's formula [26–32].

3.2 Vibrational Properties

FT-IR spectrum of WGLLE mediated CuONPs is represented in Fig. 4. The broad peak at 3840 is credited to the stretching vibration of aromatic phenolic (− OH) compounds. The bands at 3242 cm^{-1} can be allied with asymmetric stretching of the C-H band of alkanes. The peak assigned at 1687 cm^{-1}

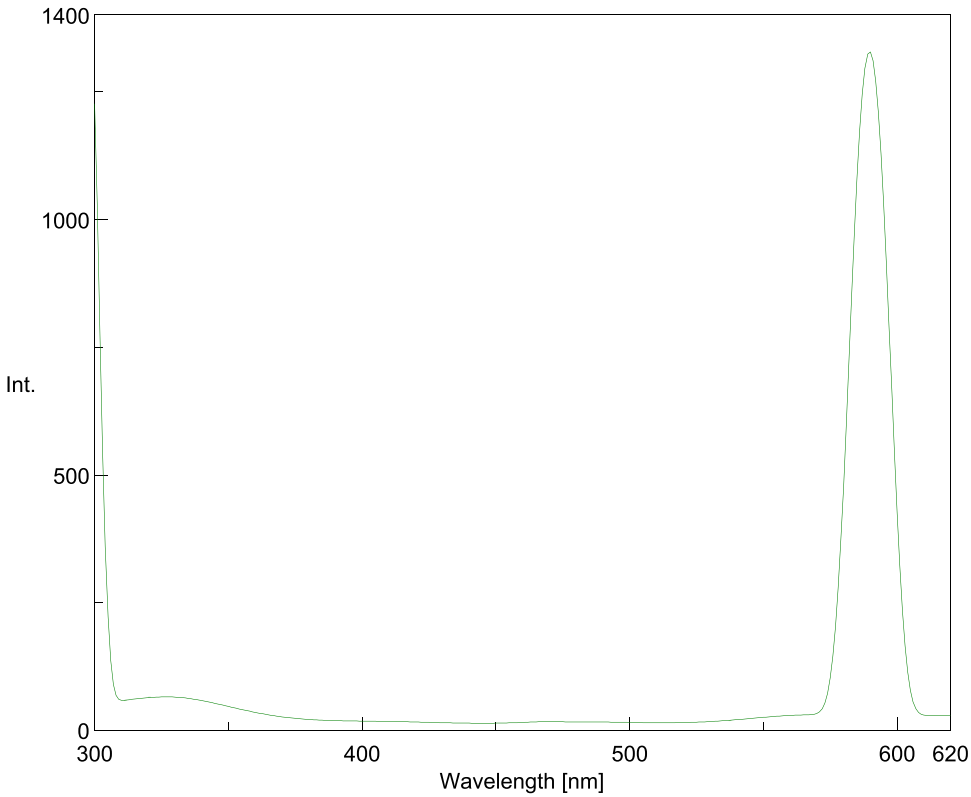

Fig. 9 PL spectra of synthesized CuONPs

Table 1 Phytochemical testing of WGLLE

Phytoconstituents	Test results
Flavonoids	P
Phenols	P
Steroids	P
Alkaloids	Ab
Tannins	Ab
Glycosides	P
Terpenoids	P
Quinones	Ab

P, presence of phytoconstituents; *Ab*, nonappearance of phytoconstituents

is due to the carbon–carbon double bond stretching frequency of polyphenol confirming the aromatic compounds. The peaks at 619 cm^{-1} and 518 cm^{-1} prove the formation of metal oxide, i.e., Cu–O, resulted of Cu–O bond stretching [33]. The FT-IR results support the existence of biomolecules as detected by phytochemical screening.

3.3 FESEM-EDAX Study

The intention of this analysis was to decide the structure along with the morphology of synthesized material. The FESEM images in Fig. 5 supports the XRD analysis as particle size range from 30 to 95 nm with a quasi-spherical shape.

The purity and chemical constituents of CuONPs were depicted by EDAX spectra shown in Fig. 6, which state that, the CuONPs are comprised of mainly Cu and O along with other elements S, K, C, Mg, Si, and P attributed to biomolecules associated with CuONPs stating crystallinity of the synthesized nanomaterial [34].

3.4 HRTEM Analysis

Figure 7 shows proof of the non-aggregated spherical, crystalline, and monoclinic nature of WGLLE-mediated CuONPs. The particle size ranges between 2–50 nm, well in agreement with XRD study.

3.5 UV–Visible Study

The wavelength of 200–800 nm was the range to record the UV–visible spectra of CuONPs as depicted in Fig. 8. The absorbance around 300 nm is a clear indication of the establishment of CuONPs, attributed to the charge transition from valence band to conduction band (O^{2-} to Cu^{2+} ion) [8].

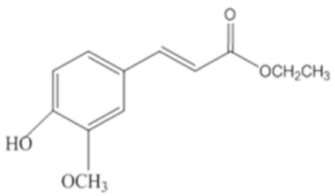

4-Hydroxy-3-methoxyethyl cinnamate

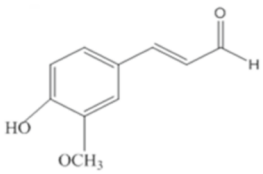

4-Hydroxy-3-methoxycinnamaldehyde

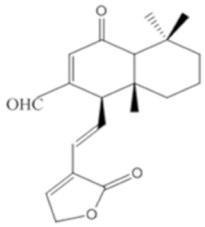

6-Oxo-7,11,13-labdatriene-17-al-16,15-olide

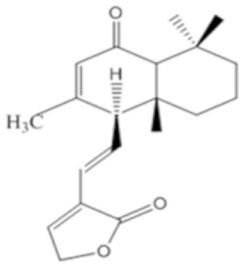

6-Oxo-7,11,13-labdatriene-16,15-olide

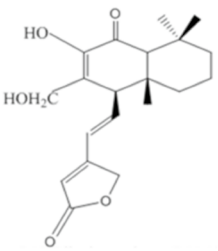

7,17,Dihydroxy-6-oxo-7,11,13-labdatrien-16,15-olide

Fig. 10 Important biomolecules in WGLLE

3.6 Photoluminescence Study

The PL spectrum was recorded in the 280–601 nm range. Figure 9 shows the luminescence character of WGLLE-mediated CuONPs as the emission bands appear at 295 and 590 nm, indicating green-yellow emission at an excitation wavelength of 290 nm. The first peak is attributed to band edge emission while the second one corresponds to the artifact. Furthermore, the Stokes pattern can be observed as the emission peak at 579 nm is twofold of excitation wavelength, i.e., 290 nm [8, 9].

3.7 Phytochemical Screening of WGLLE

Table 1 represents the biomolecules existing in the WGLLE. These important phytochemicals are capable to act as natural reducing cum capping agents in the eco benign synthesis of CuONPs [35]. Furthermore, the existence of these biomolecules had been confirmed by FT-IR spectra. Figure 10 shows important molecules reported in WGLLE.

3.8 Possible Growth Mechanism of CuONPs

The molecules representing Fig. 10 are considered for working as natural stabilizing and reducing agents in the phytofabrication of CuONPs [8, 36].

Figure 11 represents the possible growth mechanism of CuONPs. Initially, active site of WGLLE gets bound with Cu^{2+} which later being reduced to Cu^0. This Cu^0 on oxidation leads to CuONPs.

3.9 Antibacterial Activity

The antibacterial efficiency of the WGLLE-led CuONPs is tabulated in Table 2. The CuONPs showed outstanding antibacterial activities versus *E. coli and S. pyogenus* and reasonable bactericidal properties versus *S. aureus* and *P. aeruginosa* concerning reference drug ampicillin.

3.10 Antifungal Activity

The antifungal efficacy of CuONPs phytofabricated from WGLLE is shown in Table 3. The fungal strains *Aspergillus*

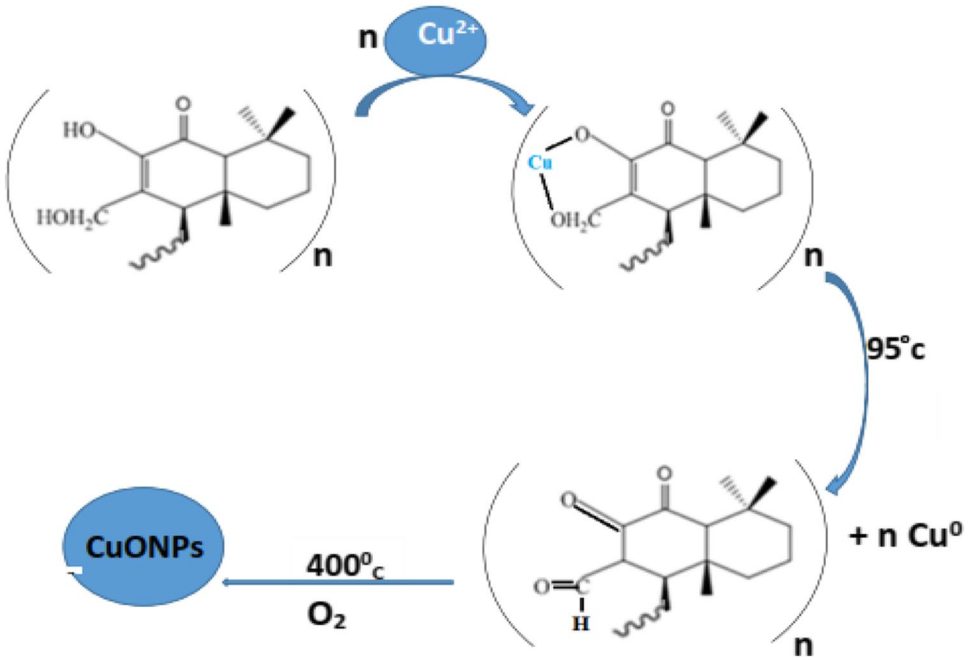

Fig. 11 Plausible mechanism of growth of CuONPs

Table 2 MIC of CuONPs against bacteria

Test pathogens	MIC (µg/ml) of CuONPs	MIC (µg/ml) of Ampicillin	MIC (µg/ml) of Ciprofloxacin
S. aureus (MTCC-96)	250	250	50
E. coli (MTCC-443)	100	100	25
P. aeuruginosa (MTCC-1688)	250	100	25
S. pyogenus (MTCC-442)	125	100	50

Table 3 MIC of CuONPs against fungi

Test pathogens	MIC (µg/ml) of CuONPs	MIC (µg/ml) of Griseofulvin	MIC (µg/ml) of Nystatin
C. albicans (MTCC-227)	1000	500	100
A. niger (MTCC-282)	500	100	100
A. clavatus (MTCC-1323)	500	100	100

niger and *Aspergillus clavatus* showed reasonable antifungal activities while the *Candida albicans* showed lower activity versus CuONPs concerning griseofulvin and nystatin as reference drugs.

3.11 Photocatalytic Activity

The photocatalytic activities of CuONPs were tested towards photodegradation of MB under sunlight using 1.0 g/dm^3 of CuONPs. Figures 12 and 13 show the decreasing concentration of MB versus time.

The decomposition rate of dye concentration versus irradiation time is presented in Fig. 14. Initially, the blank experiment was conducted without adding a photocatalyst (photolysis). The degradation rate without catalyst was negligible; but on adding photocatalyst, the concentration of the MB gradually decreased under the sunlight and 100% degradation was achieved after 70 min.

The optimization of catalyst amount from 0.1 to 1.0 g/dm^3 helped to achieve 100% degradation in 70 min. But a further increase in the amount of photocatalyst above 1.0 g/dm^3 decreased the efficiency, attributed to the aggregation of photocatalyst [37, 38].

Table 4 displays the comparison of photocatalytic potency of CuONPs with reported literature [39–42]. The data reveals the superiority of WGLLE-mediated CuONPs as a photocatalyst.

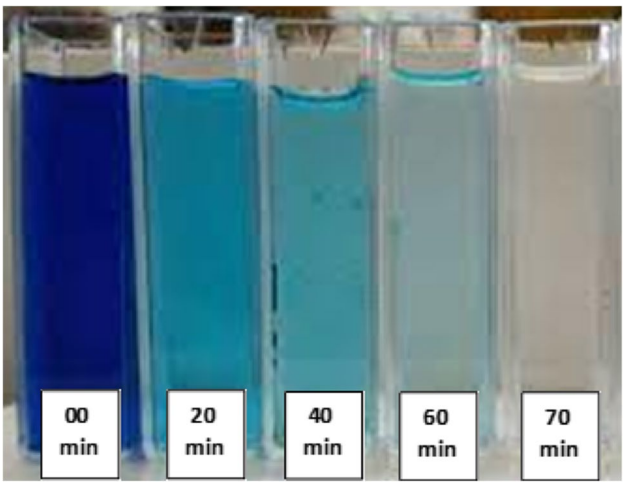

Fig. 12 Images of photodegradation of MB with respect to time

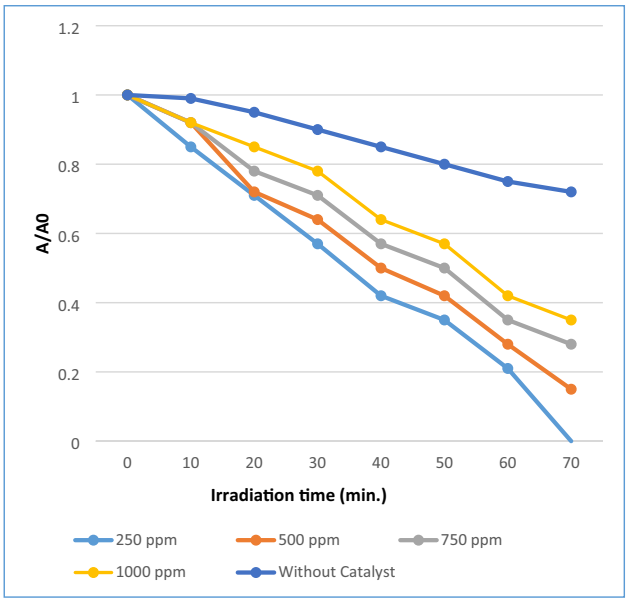

Fig. 13 A plot of A/A0 with time for the photodegradation of MB

4 Conclusion

The present article has been devoted to synthesizing CuONPs using WGLLE. The method reported for synthesis follows green chemistry ethics leading to an eco-balancing, sustainable and simple pathway. The synthesized CuONPs were characterized using basic and modern analytical tools like UV–visible spectra, XRD, FT-IR, FESEM-EDAX, HRTEM, and PL, and exhibited excellent antibacterial activities with reasonable antifungal potency against selected

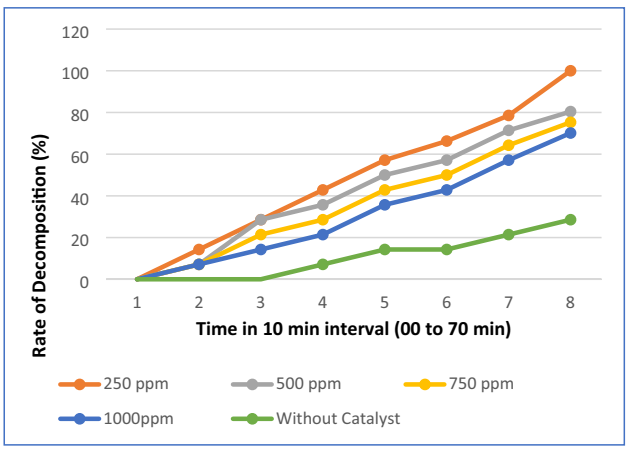

Fig. 14 Rate of decomposition of MB by using CuO NP

Table 4 Comparison of photocatalytic efficacy of phytofabricated CuONPs with recent literature

Sr. no	Materials	Plant used	Dye pollutant	Irradiation source	Degradation time (Min)	Degradation efficiency (%)	References
1	CuONPs	*Leucophyllum frutescens*	Methylene blue	Sunlight	120	88%	[39]
2	CuONPs	*Bergenia ciliata*	Methylene blue	Sunlight	135	92–85%	[40]
3	CuONPs	*Elaeagnus indica*	Methylene blue	Sunlight	360	76%	[41]
4	CuONPs	*Camellia sinesis*	Methylene blue	Sunlight	180	85.5%	[42]
5	CuONPs	*Prunus africana*	Methylene blue	Sunlight	180	83.2%	[42]
6	CuONPs	*Hedychium coronarium* Koenig	Methylene blue	Sunlight	70	100%	Present Work

bacterial and fungal pathogens. This can lead to the development of antibacterial drugs while luminescent character can turn useful in optical materials, after a detailed investigation.

Moreover, 100% degradation of MB was achieved within 70 min using novel CuONPs under sunlight. This indicates that this material can be a very good photocatalyst for the detoxification of MB dye.

Acknowledgements The authors are grateful to Instrumentation Centre, P.A.H. Solapur University, Solapur, CRNTS, IIT Bombay, IIT Madras, Jaysingpur College Jaysingpur, and Microcare Lab., Gujarat for the support in technical, instrumental, and biological activities.

Author Contribution PN put forth an idea. PN, AG, and KM carried out laboratory work. AS helped in plant recognition. PN and KM prepared the manuscript and finalized it concerning AG and AS. Finally, KM communicated to the journal.

Data Availability Data will be made available on reasonable request.

Declarations

Conflict of Interests The authors declare no competing interests.

References

1. Strathdee, S. A., Davies, S. C., & Marcelin, J. R. (2020). Confronting antimicrobial resistance beyond COVID-19 pandemic and US election. *The Lancet, 396*(10257), 1050–1053.
2. O' Neill, J. (2016). Tackling drug resistant infections globally: Final report and recommendations –the review on antimicrobial resistance chaired by Jim O' Neill, Wellcome Trust; HM Government London, UK. https://amr-review.org/sites/default/files/160525_Final%20paper_with%20cover.pdf
3. Vijayraghavan, K., & Ashokkumar, T. (2017). Plant-mediated biosynthesis of metallic nanoparticles: A review of literature, factors affecting synthesis, characterization techniques and applications. *Journal of Environmental Chemical Engineering, 5*(5), 4866–4883.
4. Marslin, G. (2018). Secondary metabolites in the green synthesis of metallic nanoparticles. *Materials, 11*, 940.
5. Ghotekar, S., Dabhane, H., Tambade, P., & Medhane, V. (2021). Chapter 9- Plant -based green synthesis and applications of cuprous oxide nanoparticles. *Handbook of Greener Synthesis of Nanomaterials and Compounds, 2*, 201–208.
6. Pagar, T., Ghotekar, S., Pagar, K., Pansambal, S., & Oza, R. (2021). Phytogenic synthesis of manganese dioxide nanoparticles using plant extracts and their biological application. *Handbook of Greener Synthesis of Nanomaterials and Compounds, 2*, 209–218.
7. Ghotekar, S., Pagar, K., Pansambal, S., H.C. Murthy, A., Oza, R. (2021). Biosynthesis of silver sulfide nanoparticles and its applications. *Handbook of Greener Synthesis of Nanomaterials and Compounds, 2*, 191–200
8. Pravinkumar Nagore, S., Ghotekar, K., Mane, A., Ghoti, M., & Bilal, A. R. (2021). Structural properties and antimicrobial activities of *Polyalthia longifolia* leaf mediated CuO nanoparticles. *BioNanoScience*. https://doi.org/10.1007/s12668-021-00851-4
9. Pansambal, S., Deshmukh, K., Savale, A., Ghotekar, S., Pardeshi, O., & Jain, G. (2017). Phytosynthsis and biological activities of fluorescent CuO nanoparticles using *Acanthospermum hispidium* L. extract. *Journal of Nanostructure, 7*(3), 165–174.
10. Reddy, C. V., Neelkanta Reddy, I., Ravindranadh, K., Reddy, K. R., Shetti, N. P., Kim, D., & Aminabhavi, T. M. (2020). Copper-doped ZrO2 nanoparticles as high-performance catalysts for efficient removal of toxic organic pollutants and stable solar water oxidation. *Journal of Environmental Management, 260*, 110088.
11. Gawande, M. B., Goswami, A., Felpin, F. X., Asefa, T., Huang, X., Silva, R., Zou, X., Zboril, R., & Varma, R. S. (2016). Cu and Cu based nanoparticles: Synthesis and applications in catalysis. *Chemical Reviews, 116*(6), 3722–3811.
12. Mohsenzadeh, J. K. S. (2015). Rapid, green, and eco-friendly biosynthesis of copper nanoparticles using flower extract of aloe vera. *Synthesis and Reactivity in Inorganic and Metal-Organic, 45*, 895–898.
13. Kolekar, R., Bhade, S., Kumar, R., Reddy, P., Singh, R., & Pradeepkumar, K. (2015). Biosynthesis of copper nanoparticles using aqueous extract of *Eucalyptus* sp. plant leaves. *Current Science, 109*(2), 255–257.
14. Rajivgandhi, G., Maruthupandy, M., Muneeswaran, T., Ramachandra, G., Manoharan, N., Quero, F., Anand, M., & Song, J. M. (2019). Biogenically synthesized copper oxide nanoparticles enhanced intracellular damage in ciprofloxacin-resistant ESBL producing bacteria. *Microbial Pathogenesis, 127*, 267–276.
15. Din, M. I., Arshad, F., Hussain, Z., & Mukhtar, M. (2017). Green adeptness in the synthesis and stabilization of copper nanoparticles: Catalytic, antibacterial, cytotoxicity, and antioxidant activities. *Nanoscale Research Letters, 12*, 638.
16. Bisht, N. S., & Bhandari, S. (2012). In vitro plant regeneration from seedling explants of *Hedychium coronarium. Journal of Medicinal Plants Research, 6*(43), 5546–5551.
17. Nagore, P. B., Lokhande, P. B., & Mujawar, H. A. (2022). Potent medicinal applications of essential oil of *Hedychium coronarium* Koenig species from the Konkan region. *Natural Volatiles Essential Oils, 9*(2), 255–261.

18. Thomas, S., Britto, S. J., Mathew, S., & Mani, B. (2014). Evaluation of antibacterial potential of silver nanoparticles produced using rhizome extract of *Hedychium coronarium* J. Koenig. *International Journal of Pharmacy and Pharmaceutical Sciences, 6*(10), 92–95.
19. Almeida M. R. (2009). Flora of Maharashtra, Vol. V A & B, Orient Press, Mumbai.102–104.
20. Fransworth, N. R. (1996). Biological and phytochemical screening of plants. *Journal of Pharmaceutical Sciences, 55*, 225–227.
21. Rattan, A. (2000). Antimicrobials in laboratory medicine. Churchill B. I., Livingstone, New Delhi. 85–108.
22. Wiegand, I., Hilpert, K., & Hancock, R. E. W. (2008). Agar and broth dilution methods to determine the minimal inhibitory concentration (MIC) of antimicrobial substances. *Nature Protocols., 3*, 163–175.
23. Alvand, Z. M., Rajabi, H. R., Mirzaei, A., & Masoumisl, A. (2019). Ultrasonic and microwave assisted extraction as rapid and efficient techniques for plant mediated synthesis of quantum dots: Green synthesis, characterization of zinc telluride and comparison study of biological activities. *New Journal of Chemistry, 43*, 15126–15138.
24. Sharma, P., Pant, S., Dave, V., Tak, K., Sadhu, V., & Reddy, K. R. (2019). Green synthesis and characterization of copper nanoparticles by *Tinospora cardifolia* to produce nature-friendly copper nano-coated fabric and their antimicrobial evaluation. *Journal of Microbiol Methods, 160*, 107–116.
25. Misra, A., Jain, S., Kishore, D., Dave, V., Reddy, K. R., Sadhu, V., Dwivedi, J., & Sharma, S. (2019). A facile one pot synthesis of novel pyrimidine derivatives of 1,5benzodiazepines via domino reaction and their antibacterial evaluation. *Journal of Microbiol Methods, 163*, 105648.
26. Patterson, A. (1939). The Scherrer formula for X-ray particle size determination. *Physical Review, 56*, 978–982.
27. Mane, K. G., Nagore, P. B., & Pujari, S. R. (2018). Synthesis, photophysical, electrochemical and thermal investigation of anthracene doped 2-Naphthol Luminophors and their thin film for optoelectronic devices. *Journal of Fluorescence, 28*(5), 1023–1028.
28. Mane, K. G., Nagore, P. B., & Pujari, S. R. (2019). Synthesis of highly fluorescent D-A based p-terphenyl luminophors and their thin films for optoelectronic applications. *Journal of Fluorescence, 29*(4), 1001–1006.
29. Mane, K. G., Nagore, P. B., & Pujari, S. R. (2019). Novel 2-naphthol luminophors for optoelectronics. *Applied Physics A, 125*(10), 729.
30. Mane, K. G., Nagore, P. B., & Pujari, S. R. (2019). Synthesis of novel blue and green light emitting 4-nitrophenol luminophors for optoelectronics. *Journal of Fluorescence, 29*(6), 1371–1380.
31. Mane, K. G., Nagore, P. B., & Pujari, S. R. (2020). Photophysical and structural aspects of perylene doped 2-naphthol luminophors: Green emission by exciplex formation. *Luminescence, 35*(2), 292–298.
32. Pujari, S. R., Nagore, P. B., Ghoti, A. J., & Mane, K. G. (2021). Novel donor-acceptor based 2-naphthol luminophors as hole-transporting materials for optoelectronics. *Journal of Fluorescence, 31*(1), 259–267.
33. Sone, B. T., Diallo, A., Fuku, X. G., Gurib-Fakim, A., & Maaza, M. (2017). Biosynthesized CuO nano-platelets: Physical properties and enhanced thermal conductivity nanofluidics. *Arabian Journal of Chemistry, 13*(1), 160–170. https://doi.org/10.1016/j.arabjc.2017.03.004
34. Tamuly, C., Saikia, I., Hazarika, M., & Das, M. R. (2014). Reduction of aromatic nitro compounds catalyzed by biogenic CuO nanoparticles. *RSC Advances, 4*, 53229.
35. Pachurekar, P., & Dixit, A. K. (2017). A review on pharmacognostical phytochemical and ethnomedicinal properties of *Hedychium coronarium* J.Koenig an endangered medicine. *International Journal of Chinese Medicine, 1*(2), 49–61.
36. Siddiqui, H., Qureshi, M. S., & Haque, F. Z. (2014). One-step, template- free hydrothermal synthesis of CuO tetrapods. *Optik, 125*(17), 4663–4667.
37. Gawade, V. V., Gavadem, N. L., Shinde, H. M., Babar, S. B., Kadam, A. N., & Garadkar, K. M. (2017). Green synthesis of ZnO nanoparticles by using *Calotropis procera* leaves for the photodegradation of methyl orange. *Journal of Materials Science: Materials in Electronics, 28*, 140033–140039. https://doi.org/10.1007/s10854-017-7254-2
38. Bhosale, R. R., Pujari, S. R., Muley, G. G., Patil, S. H., Patil, K. R., Shaikh, M. F., & Gambhire, A. B. (2014). Solar photocatalytic degradation of methylene blue using doped TiO2 nanoparticles. *Solar Energy, 103*, 473–479.
39. Ahmad, A., Khan, M., Khan, S., Luque, R., Abualnaja, K. M., Alduaij, O. K., & Yousef, T. A. (2022). Bio-construction of CuO nanoparticles using Texas sage plant extract for catalytical degradation of methylene blue. *Journal of Molecular Structure, 1256*, 132522. https://doi.org/10.1016/j.molstruc.2022.132522
40. Kosarsoy-Agceli, G., Dulta, K., Chauhan, P. K., & Chauhan, P. (2022). Multifunctional CuO nanoparticles with enhanced photocatalytic dye degradation and antibacterial activity. *Sustainable Environment Research, 32*(1), 1–15. https://doi.org/10.1186/s42834-021-00111-w
41. Indira, D., Krishnamoorthy, M., Ameen, F., Bhat, S. A., Amurgum, K., Ramalingam, S., Priyan, S. R., & Kumar, G. S. (2022). Biomimetic facile synthesis of zinc oxide and copper oxide nanoparticles from *Elaeagnus indica* for enhanced photocatalytic activity. *Environmental Research, 212*, PartC, 113323. https://doi.org/10.1016/j.envres.2022.113323
42. Ssekatawa, K., Byrugawa, D. K., Angwe, M. K., Wampande, E. M., Ejobi, F., Nxumalo, E., Maaza, M., Sackey, J., & Kirabira, J. B. (2022). Phyto-mediated copper oxide nanoparticles for antibacterial, antioxidant and photocatalytic performances. *Frontiers in Bioengineering & Biotechnology* 10, 820218. https://doi.org/10.3389/2Ffbioe.2022.820218